

LETTER • OPEN ACCESS

Increasing risk of compound wind and precipitation extremes due to tropical cyclones in India

To cite this article: Akshay Rajeev and Vimal Mishra 2023 *Environ. Res.: Climate* **2** 021004

View the [article online](#) for updates and enhancements.

You may also like

- [Differences in the destructiveness of tropical cyclones over the western North Pacific between slow- and rapid-transforming El Niño years](#)
Shifei Tu, Jianjun Xu, Feng Xu et al.
- [Storm surge variability and prediction from ENSO and tropical cyclones](#)
Yicheng Tan, Wei Zhang, Xiangbo Feng et al.
- [Predicting compound coastal inundation in 2100 by considering the joint probabilities of landfalling tropical cyclones and sea-level rise](#)
Y Peter Sheng, Kun Yang and Vladimir A Paramygin

ENVIRONMENTAL RESEARCH CLIMATE



LETTER

Increasing risk of compound wind and precipitation extremes due to tropical cyclones in India

OPEN ACCESS

RECEIVED

22 September 2022

REVISED



17 April 2023

ACCEPTED FOR PUBLICATION

21 April 2023

PUBLISHED

11 May 2023

Akshay Rajeev¹  and Vimal Mishra^{1,2,3,*} ¹ Earth Sciences, Indian Institute of Technology (IIT) Gandhinagar, Gandhinagar, Gujarat, India² Civil Engineering, Indian Institute of Technology (IIT) Gandhinagar, Gandhinagar, Gujarat, India³ Kiran C Patel Center of Sustainable Development, IIT Gandhinagar, Gandhinagar, Gujarat, India

* Author to whom any correspondence should be addressed.

E-mail: vmishra@iitgn.ac.in**Keywords:** compound extremes, wind extremes, precipitation extremes, tropical cycloneSupplementary material for this article is available [online](#)

Original content from this work may be used under the terms of the [Creative Commons Attribution 4.0 licence](#).

Any further distribution of this work must maintain attribution to the author(s) and the title of the work, journal citation and DOI.



Abstract

Tropical cyclones (TCs) cause compound extremes of rainfall and wind gust. However, their occurrence and impacts on India still need to be better understood. Using ERA5 reanalysis and cyclone eAtlas, we examine the compound extremes of precipitation and wind gust driven by TCs that made landfall over India during 1981–2021. Based on the joint return period of compound extremes, the five worst TCs occurred in May 1990, May 1999, May 2010 (Laila), October 2014 (Hudhud), and May 2020 (Amphan). A majority of TCs during 1981–2021 originated from the Bay of Bengal (BoB) and only a few from the Arabian Sea (AS). While the frequency of all the TCs has either declined or remained stable in the North Indian Ocean (NIO, BoB, AS) during 1981–2021, the frequency of TCs with compound extremes has increased by about three-fold during the most recent decade (2011–2021). Compound extremes driven by TCs affect large regions along the coast and risk infrastructure and human lives. The frequency of TCs with large area of impact (greater than 200 000 km²) compound wind and precipitation extreme extent exhibits a three-fold rise during 1981–2021, indicating an increase in the hazard associated with the compound extremes driven by TCs in India.

1. Introduction

Compound events occur when two or more weather or climate extremes co-occur, in close succession, or concurrently in different regions, leading to impacts more significant than that due to individual events (Seneviratne *et al* 2012). Compound events can be grouped into preconditioned, multivariate, and temporally and spatially compounding (Zscheischler *et al* 2020). Precondition events include flooding caused by significant rainfall and high soil moisture conditions (Martius *et al* 2013, Grams *et al* 2014, Garg and Mishra 2019). On the other hand, compound flooding during storms (Bevacqua *et al* 2019, Hendry *et al* 2019) and concurrent precipitation and wind extremes (Raveh-Rubin and Wernli 2015, Martius *et al* 2016) can be considered multivariate events. Temporal clustering of storms and precipitation events are temporally compounding events (Mailier *et al* 2006, Barton *et al* 2016), while co-occurrence of drought and heatwave leading to crop failure can be considered as spatially compounding events (Singh *et al* 2018, Anderson *et al* 2019).

Compound wind and precipitation extremes have received considerable attention in the recent past (Raveh-Rubin and Wernli 2015, Messmer and Simmonds 2021, Zhang *et al* 2021, Zscheischler *et al* 2021). Often, a single weather system, such as a tropical cyclone (TC) or an extratropical cyclone, triggers simultaneous precipitation and wind extremes over a region (Rodgers and Pierce 1995, Raveh-Rubin and Wernli 2015). Most compound wind and precipitation extremes affect coastal regions and areas frequently affected by TCs (Seneviratne *et al* 2021). Annually, India is affected by TCs originating in the North Indian Ocean (NIO) and causing significant damage to life and infrastructure. These impacts are likely to rise due to

climate change as the frequency and intensity of TCs are likely to enhance (Knutson *et al* 2010, Walsh *et al* 2015). Seneviratne *et al* (2021) reported high confidence in increased precipitation and high wind speed associated with TCs under multiple scenarios.

Despite being prone to TCs-driven compound wind and precipitation extremes, the occurrence and impact of such events over India remain unexplored. Here, we aim to examine India's compound wind and precipitation extremes associated with TCs. We address the questions: (1) how has the occurrence and extent of wind and precipitation compound extremes changed over time? and (2) Does TC-induced compound wind, and precipitation extremes affect a substantial region over India compared to the individual extremes? We estimate the joint return period of TC-induced compound wind and precipitation extremes from 1981 to 2021 using the Cyclone eAtlas from India Meteorological Department (IMD) and the ERA5 reanalysis. We evaluate the interdecadal variation in the frequency of TCs with compound extremes and that for TCs with large compound extreme extent from 1981 to 2021. Additionally, based on the joint return period, we select the five most severe TCs during 1981–2021 and evaluate the spatial distribution of precipitation, wind, and their compound extremes.

2. Data and methods

2.1. Data

As we aim to examine compound extremes of TC-induced rainfall and wind extremes over the Indian region, we used the ERA5 reanalysis dataset, which provides continuous hourly data from 1979 onwards. The European Centre developed the ERA5 reanalysis dataset for Medium-Range Weather Forecasts. We obtained hourly total precipitation and 10 m instantaneous wind gust at 31 km spatial resolution for the Indian region. The daily accumulated precipitation was estimated from the hourly precipitation and the daily mean wind gust from the instantaneous hourly wind gust. The availability of continuous data and the different variables at a high resolution from the ERA5 is vital for assessing the wind and precipitation extremes associated with each TC. Recent studies employed the ERA5 reanalysis to analyze wind and precipitation compound extremes (Messmer and Simmonds 2021, Owen *et al* 2021, Zscheischler *et al* 2021).

We extracted the TC tracks from the Cyclone eAtlas of IMD, which is an electronic atlas of the cyclonic disturbances (CD) in the NIO and provides data from 1891 to 2020 (Cyclone eAtlas-IMD 2021). The atlas provides tracks of CDs of three categories based on sustained wind speeds, including depressions (D) [$31\text{--}51\text{ km h}^{-1}$], cyclonic storms (CS) [$62\text{--}87\text{ km h}^{-1}$], and severe cyclonic storms (SCS) [$88\text{--}117\text{ km h}^{-1}$]. IMD further divided the SCS category based on sustained wind speeds. We used TCs, which according to the TC classification of IMD, fall under the following categories: CS, SCS, very severe cyclonic storms (VSCS) [$118\text{--}165\text{ km h}^{-1}$], extremely severe cyclonic storms (ESCS) [$166\text{--}221\text{ km h}^{-1}$], and super cyclonic storms (SuCS) [$\geq 221\text{ km h}^{-1}$]. VSCS, ESCS and SuCS correspond to very high wind speeds and can potentially be devastating as they make landfall. We only considered TCs that made landfall over India during 1981–2021. In addition to the Cyclone eAtlas, we also used the IMD best track data for the tracks of the 2021 TCs.

2.2. Methods

2.2.1. Defining area affected by TCs

We used the cyclone tracks to estimate each TC event's duration and landfall dates. Since we aim to understand the severity of TC-induced compound precipitation and wind extremes, we selected an area along its path over land where the TC made landfall for each event. The spatial distribution of TC rainfall and its variation can differ from the cyclone's wind gust for an event (Kimball 2008, Matyas 2010). Considering the entire area affected by TC might result in an underestimation of extreme rainfall associated with the TC, as currently, TC size is determined by wind structures (Kim *et al* 2019). Since the focus is on compound extremes, we used an area of approximately $35\,000\text{ km}^2$ where both wind and precipitation extremes have occurred during each TC, rather than considering the entire TC-affected region. We estimated the area-averaged long-term (1981–2021) daily rainfall and mean wind gust for the selected region affected by the compound extremes. The uniformity in the areal extent considered for each TC helps us compare different TCs, as TC size varies with the environmental conditions associated with each event (Kim *et al* 2019). In addition to the areal extent of $35\,000\text{ km}^2$, we repeated the methodology for areal extents of $15\,000\text{ km}^2$, $60\,000\text{ km}^2$ and $95\,000\text{ km}^2$ to determine the robustness of our results (figure S1).

2.2.2. Definition of extreme precipitation, wind gust and compound events

We used the standardized precipitation and wind gust anomalies to estimate the spatial distribution of extreme precipitation and wind gust during each event. Both precipitation and wind gust were standardized for each grid over the 1981–2021 period. For example, the climatology of grid A is used to estimate the standard deviation of precipitation and wind gust of grid A and the climatology of grid B is used to estimate

the standard deviation of variables of grid B. We also estimated the region affected by compound extremes of precipitation and wind gust during each event by calculating the grid points where the standard deviation of precipitation and wind gust exceeds three. We used standard deviation three as the threshold to estimate the region affected by compound extremes because it corresponds to the 99.7th percentile values of wind and precipitation. Percentile-based thresholds of extremes are frequently used for analyzing climate extremes and are known as moderate extremes (Zhang *et al* 2011). Martius *et al* (2016) used a 98th percentile threshold to quantify global co-occurring precipitation and wind extremes and argued that moderate extremes cause significant societal and environmental damage. Similarly, Klawns and Ulbrich (2003) showed that wind speeds corresponding to 98th percentile values could cause severe damage. In many regions, 24 hour precipitation corresponding to the 98th percentile can trigger landslides and debris flow (Guzzetti *et al* 2008). Hence, TC precipitation and wind greater than the 99.7th percentile (standard deviation >3) can cause a significant impact.

We used the precipitation and wind gust anomaly. We considered extreme wind as the area having wind gusts and precipitation anomalies exceeded three standard deviations in examining the interdecadal variation in spatial extent. The area affected by compound wind and precipitation extreme is taken as the region where both precipitation and wind anomaly exceed three. We estimated the area affected by extreme wind, precipitation, and compound extremes during each TC in the NIO for the 1981–2021 period (table S2). Moreover, we estimated the TC area for extreme wind gust, precipitation, and their compound extremes on the day before landfall as TC size reduces after the landfall. We also used the threshold of 200 000 km² to identify TCs with large areal extent. The area of 200 000 km² corresponds to a diameter of approximately 500 km if a circular extent is assumed. According to the World Meteorological Organization 2020, the diameters of TCs are typically around 200–500 km and can reach up to 1000 km. Therefore, we selected the area corresponding to the upper limit of the size of a typical TC as the threshold.

2.2.3. Univariate and joint return period calculation

In addition to the percentile-based threshold, we used univariate and joint return periods to examine extremes. We obtained the area-averaged long-term (1981–2021) daily precipitation and mean wind gust associated with each TC event (see section 2.2.1). For this, we chose an area affected by the highest magnitudes of extreme rainfall and wind gust from the TC. Additionally, we prioritized the regions to be completely over land and focused on a period close to the landfalling date. We estimated the annual maximum rainfall and wind gust for each time series, the average yearly maximum rainfall and wind gust over a region. These annual maximum rainfall and wind gust are then fit to a generalized extreme value (GEV) distribution. We used the Kolmogorov–Smirnov and Anderson–Darling goodness of fit tests to assess the quality of the convergence of the GEV distribution. The null hypothesis of both tests is that the data follow the specified distribution. After the values are fit to the GEV, we estimate the return period (precipitation and wind gust) associated with the period affected by the TC. We consider a six-day period (Landfall date ± 3 d) to determine the day of peak wind gust and precipitation. These peak wind gust and precipitation associated with the TC is then used to determine the return periods. The univariate return periods of this daily rainfall and mean wind gust are estimated from the GEV distribution.

Additionally, we estimated the joint return period of peak daily precipitation and wind gust associated with each TC event by fitting a copula to the long-term data. We first transformed rainfall and wind gust to uniformly distributed marginals by fitting values to the GEV distribution. A similar methodology has been employed in previous studies to estimate joint return periods (Hao *et al* 2018, Ye and Fang 2018, Bevacqua *et al* 2020). We used four copula families from Archimedean and Elliptical copulas (Clayton, Frank, Gumbel, and Student-t), which are commonly used for analyzing hydroclimatic extremes as the candidate functions (Hao *et al* 2018, Li *et al* 2019) [table 1]. The best fit copula family changed based on marginal distributions of precipitation and wind gust associated with each TC. We selected the best-ranked family for each TC using the smallest Akaike information criterion (table S1). The copulas were fitted using a maximum-likelihood estimator [*VineCopula* R-package, Nagler *et al* 2021]]. We then estimated the joint return period of extreme precipitation and wind gust for each TC event using the:

$$T(u,v) = \frac{\mu}{1 - u - v + C(u,v)} \quad (1)$$

Here μ is the mean inter-arrival time between successive events, which was considered 1 for the annual probability. u and v are the marginal distribution of precipitation and wind gust, respectively which are obtained by fitting the values to the GEV distribution. C is the copula function. After estimating the joint return periods, we identified TCs with compound extremes with more than ten years of joint return periods. Similarly, for precipitation and wind extremes, we used a threshold of a 10 year univariate return period.

Table 1. Formulas of the copula functions and the corresponding parameter space.

Copula	$C(u, v)$	Parameter space
Clayton-copula	$(u^{-\alpha} + v^{-\alpha})$	$\alpha \geq 0$
Frank-copula	$-\frac{1}{\alpha} \ln \left(1 + \frac{(e^{-\alpha u} - 1)(e^{-\alpha v} - 1)}{(e^{-\alpha} - 1)} \right)$	$\alpha \neq 0$
Gumbel-copula	$\exp \left\{ -[(-\ln u)^\alpha + (-\ln v)^\alpha]^{1/\alpha} \right\}$	$\alpha \geq 1$
Student-t	$\int_{-\infty}^{t_v^{-1}(u)} \int_{-\infty}^{t_v^{-1}(v)} \frac{1}{2\pi(1-\alpha^2)^{3/2}} \left\{ 1 + \frac{x^2 - 2\alpha xy + y^2}{v(1-\alpha^2)} \right\}^{-(v+2)/2} dy dx$	$-1 < \alpha < 1$

Where $t_v^{-1}(\cdot)$ Denotes inverse function of the CDF $t_v(\cdot)$
 α is between $t_v^{-1}(u)$ and $t_v^{-1}(v)$
 x and y are independent variables

3. Results

3.1. The worst TCs (1981–2021)

We selected 94 TCs that made landfall over India from 1981 to 2021 (figure 1(a)). For each of the 94 TCs, we estimated univariate and joint return periods of daily precipitation and wind gust (table S1). We selected the top five TC events, having the highest joint return period that has affected India during the entire period. The worst TC that affected India occurred in May 1999, which originated in the Arabian Sea (AS) with a joint return period of 596 years. However, the return period of extreme precipitation associated with this event is only five years, while the return period of the wind gust is exceptionally high. The TC event associated with the second-highest joint return period occurred in October 2014, named Hudhud. For Hudhud, the return period of extreme precipitation is 31 years, while wind gust has a return period of 211 years. The third most intense TC event in terms of joint return period occurred in May 1990, which originated in the Bay of Bengal (BoB) and had a joint return period of 126 years. The TC events with the fourth and fifth-highest return periods occurred in May 2010 TC (named Laila) and May 2020 TC (named Amphan), respectively.

3.2. Spatial distribution of the worst TCs

Next, we examine the spatial distribution of wind gust and precipitation associated with the five TCs having the highest joint return period that affected India during the 1981–2021 period. We first analyze the TC event that occurred in May 1990, which originated from the BoB and affected the Indian states of Andhra Pradesh and Tamil Nadu. The TC caused considerable property loss and affected a population of 7.78 million (RSMC 1991). Based on the peak wind gust associated with the May 1990 TC, the TC was classified as a SuCS. A large region was affected by extreme wind gust (standard deviation >3) due to the TC. However, once the TC made landfall, the area affected by extreme wind gust started to decrease. We also estimated the area-averaged wind gust during this period along the TC track (figure 2). The TC generated severe wind gust ($>20 \text{ m s}^{-1}$) over the region with a return period of 122 years. On 9 May 1990, the wind speed along the coast increased from approximately 27 m s^{-1} to a peak of 38 m s^{-1} as the TC passed over, which indicate faster winds in the rear of the TC and slower winds in the front (RSMC 1991). Subsequently, we examined the precipitation associated with the TC (figure 3). The area affected by extreme rainfall decreases as the TC moves closer to land, while extreme precipitation had a 60 year return period (180 mm) on 9 May 1990 (figure 3(e)). Additionally, rainfall due to the TC was distributed over many days, suggesting a slow translational speed. Widespread heavy rain was reported in association with the TC during 8–11 May 1990, with some stations recording a total rainfall of 1100 mm (RSMC 1991).

The spatial pattern of precipitation anomaly does not strictly follow that of the wind gust anomaly from the same TC. Moreover, a larger area is affected by a positive precipitation anomaly than the region affected by a positive wind gust anomaly. To understand the compound wind and precipitation extremes due to TCs, we estimated the area affected by extreme wind gust and precipitation (figure 4). We identified the region of compound extremes where both the standardized precipitation anomaly and wind gust anomaly are three or higher. Compound wind and precipitation extremes due to the May 1990 TC affected a large area, which reduced after the landfall. Nevertheless, compound wind and precipitation extremes affect a significant region along the coast. The joint return period associated with this event was estimated to be 126 years.

The TC event of May 1999 originated in the AS and was classified as an ESCS. The TC caused heavy rainfall in Gujarat, Rajasthan, and parts of Pakistan, leading to a severe loss of property and human lives (RSMC 2000). The distribution of wind gust anomaly indicates that the extreme wind caused by the TC was relatively low before 19 May 1999 (figure 2(a)). However, a significant area was affected by extreme wind

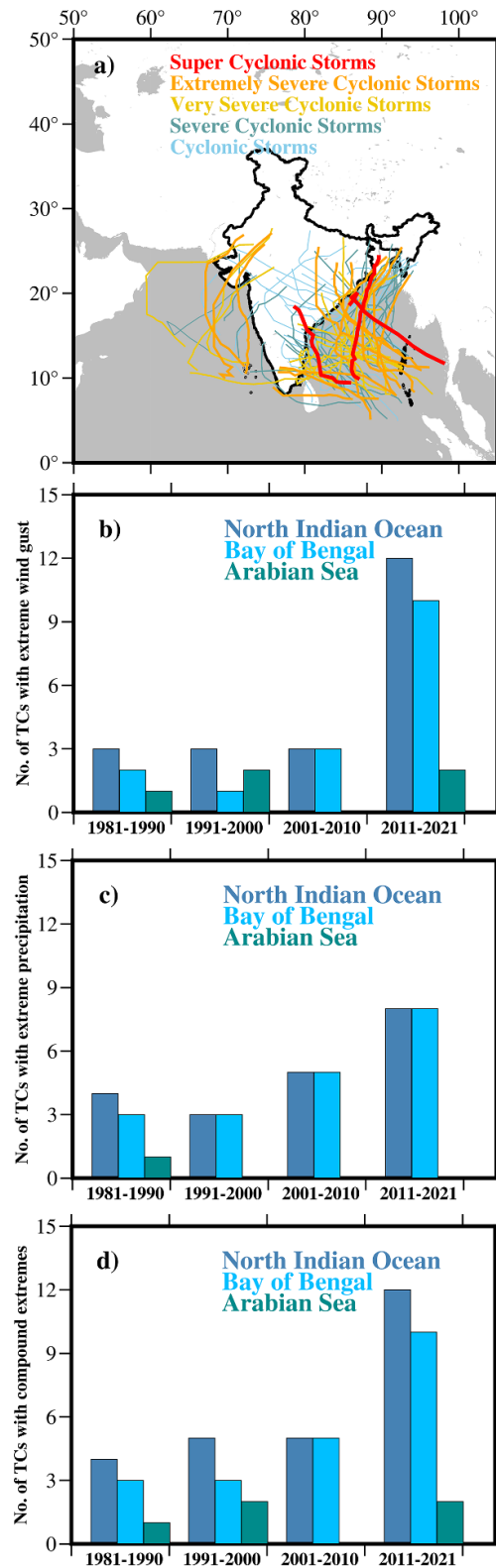


Figure 1. (a) Tracks of TCs which affected Indian region from 1981–2021. The different colors and the thickness of the tracks represent the maximum intensity of the TC where the red track represents super cyclonic storms (SuCS), the orange track represents extremely severe cyclonic storms (ESCS), the yellow track represents very severe cyclonic storms (VSCS), the green track represents severe cyclonic storms (SCS) and the blue track represents cyclonic storms (CS). (b) Interdecadal variability of TC with extreme wind gust (TC wind gust return period >10 years) for the entire NIO, BoB and AS. (c) Interdecadal variability of TC with extreme precipitation (TC precipitation return period >10 years) for the entire NIO, BoB and AS. (d) Interdecadal variability of TC with compound wind and precipitation extremes (joint return period >10 years) for the entire NIO, BoB and AS.

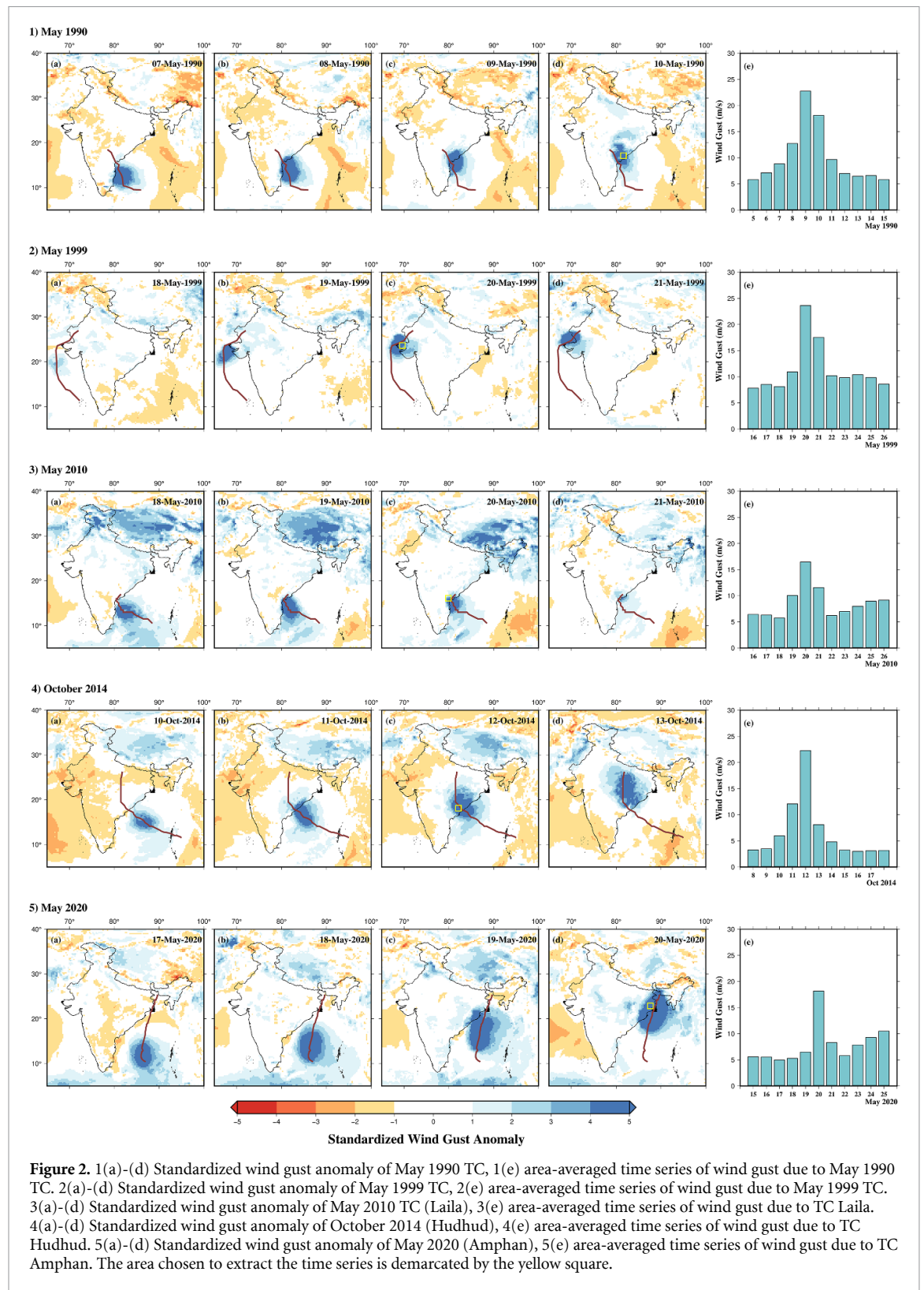


Figure 2. 1(a)-(d) Standardized wind gust anomaly of May 1990 TC, 1(e) area-averaged time series of wind gust due to May 1990 TC. 2(a)-(d) Standardized wind gust anomaly of May 1999 TC, 2(e) area-averaged time series of wind gust due to May 1999 TC. 3(a)-(d) Standardized wind gust anomaly of May 2010 TC (Laila), 3(e) area-averaged time series of wind gust due to TC Laila. 4(a)-(d) Standardized wind gust anomaly of October 2014 (Hudhud), 4(e) area-averaged time series of wind gust due to TC Hudhud. 5(a)-(d) Standardized wind gust anomaly of May 2020 (Amphan), 5(e) area-averaged time series of wind gust due to TC Amphan. The area chosen to extract the time series is demarcated by the yellow square.

during 19–21 May 1999 (figure 2(b)–(d)). Such an increase in wind gust associated with the TC can be attributed to the rapid intensification of TC as it moves north. The area-averaged wind gust for an area along the track near Kutch shows a peak wind gust of approximately 25 m s^{-1} , with an extremely high return period of 595 years, on 20 May 1999 (figure 2(e)). Such extreme TC winds on 20 May could be because the TC had not yet made landfall and had the highest intensity before making landfall the next day. The precipitation anomaly on 18 May 1999 shows a positive anomaly over a large area, which indicated that TC caused heavy rainfall even before the TC intensified to produce extreme winds (figure 3(a)). On 19–21 May 1999, the positive wind gust anomaly covered a larger area than the positive precipitation anomaly

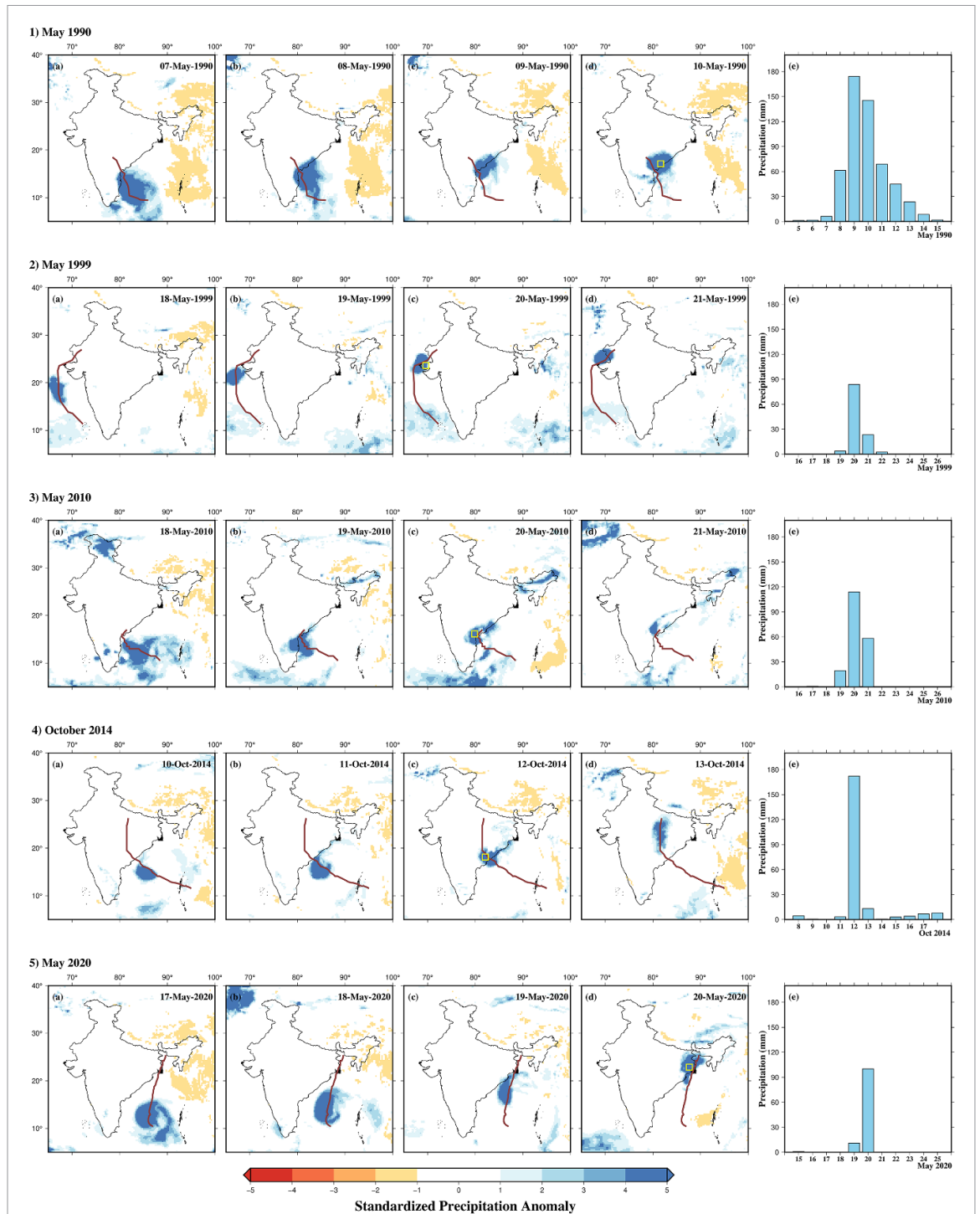
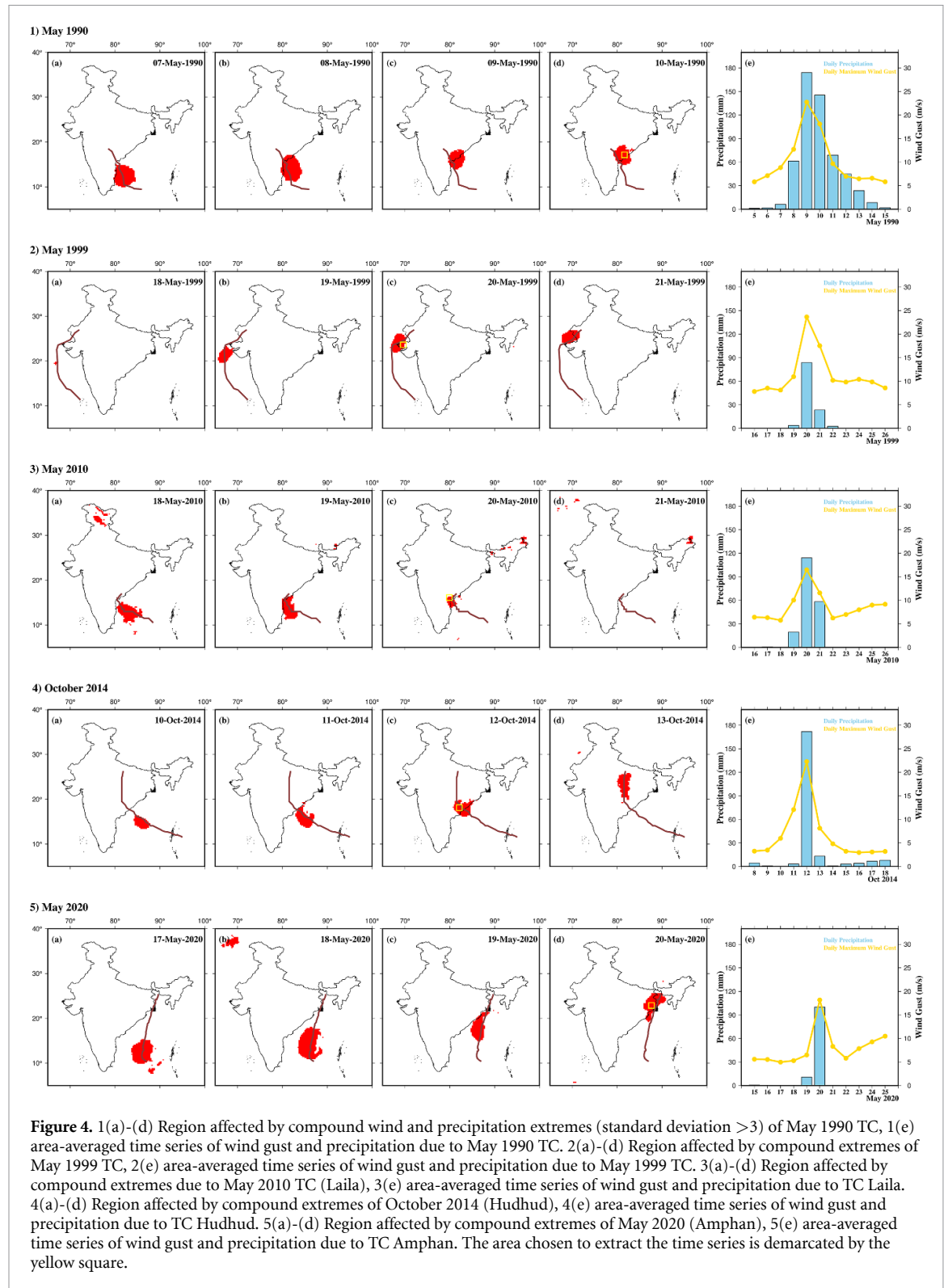


Figure 3. 1(a)-(d) Standardized precipitation anomaly of May 1990 TC, 1(e) area-averaged time series of precipitation due to May 1990 TC. 2(a)-(d) Standardized precipitation anomaly of May 1999 TC, 2(e) area-averaged time series of precipitation due to May 1999 TC. 3(a)-(d) Standardized precipitation anomaly of May 2010 TC (Laila), 3(e) area-averaged time series of wind gust due to TC Laila. 4(a)-(d) Standardized precipitation anomaly of October 2014 (Hudhud), 4(e) area-averaged time series of precipitation due to TC Hudhud. 5(a)-(d) Standardized precipitation anomaly of May 2020 (Amphan), 5(e) area-averaged time series of precipitation due to TC Amphan. The area chosen to extract the time series is demarcated by the yellow square.

(figure 3(b)–(d)). The area-averaged rainfall peaked at approximately 90 mm on 20 May 1999 (figure 3(e)). The spatial distribution of compound wind and precipitation extremes shows that only a small region was affected (figures 4(a) and S2). During the following days, a large area was affected by compound extremes (figures 4(b)–(d) and S2). The magnitude of the wind gust was higher compared to that of the precipitation (figure 4(e)). We estimated the May 1999 TC to have a joint return period of 596 years, making this the most devastating TC to affect India during the entire period.

The May 2010 TC (Laila) originated from the BoB, which was classified as an SCS and affected the Indian states of Andhra Pradesh and Tamil Nadu. The cyclone caused heavy rainfall and strong winds leading to



moderate damage (RSMC 2011). The positive wind gust anomaly associated with TC Laila was spread over a large area but quickly dissipated once it made landfall (figure 2(a)–(d)). The area-averaged peak wind gust caused by this TC near the coast was approximately 17 m s^{-1} (34 year return period) on 20 May 2010 (figure 2(e)). The positive precipitation anomaly of TC Laila affected a large region over the ocean, and its extent reduced as it moved towards land (figure 3(a)–(d)). The TC caused extreme rainfall over land more extensively than extreme wind gust. The TC caused severe area-averaged precipitation of approximately 120 mm (26 year return period) along the track near the coast on 20 May 2010 (figure 3(e)). The TC caused compound extremes over a large area along the track over the ocean. However, the area affected by

compound extremes was significantly reduced as the TC made landfall. The magnitude of area-averaged precipitation and wind gust is moderately high and has a joint return period of 88 years (figure 4(e)).

The October 2014 TC event (Hudhud), classified as an ESCS, affected North Andhra Pradesh and South Odisha with heavy rainfall and strong winds leading to severe structural damage (RSMC 2015). The region with positive wind gust anomaly due to TC Hudhud increased as it moved towards land and, even after landfall, extended further inland (figure 2(a)–(d)). The peak daily wind gust associated with this TC was high ($\sim 23 \text{ m s}^{-1}$; 211 year return period, figure 2(e)). Compared to the wind gust anomaly of TC Hudhud, the positive precipitation anomaly covers a smaller area as it moves along the track (figure 3(a)–(d)). However, it produced significant rainfall along the coast, with a peak of approximately 180 mm having a 31 year return period (figure 3(e)). The extent of compound wind and precipitation extremes due to TC Hudhud increases as it moves landward and affects a significant area overland (figure 4(a)–(d)). Additionally, we find that the magnitude of area-averaged precipitation and wind gust is high and has a joint return period of 240 years (figure 4(e)).

In May 2020, a SuCS formed in the BoB named Amphan, which affected Odisha, West Bengal, and parts of Bangladesh. TC Amphan caused heavy rainfall and winds leading to significant damage to property and life (RSMC 2021). The extent of the region with positive wind gust anomaly increased as the TC moved north and affected a large area over land. The area-averaged peak wind gust near the coast was about 18 m s^{-1} with a return period of 25 years (figure 2(e)). On the other hand, the extent of precipitation's positive anomaly was initially greater and slightly decreased as it moved towards land (figure 3(a)–(d)). Moderately heavy rainfall of 100 mm (25 year return period) was associated with TC Amphan (figure 3(e)). TC Amphan caused compound wind and precipitation extremes along the TC path and affected a significant region overland (figure 4(a)–(d)). TC Amphan had a joint return period of 71 years, and peak precipitation and wind gust associated with it were moderately high (figure 4(e)).

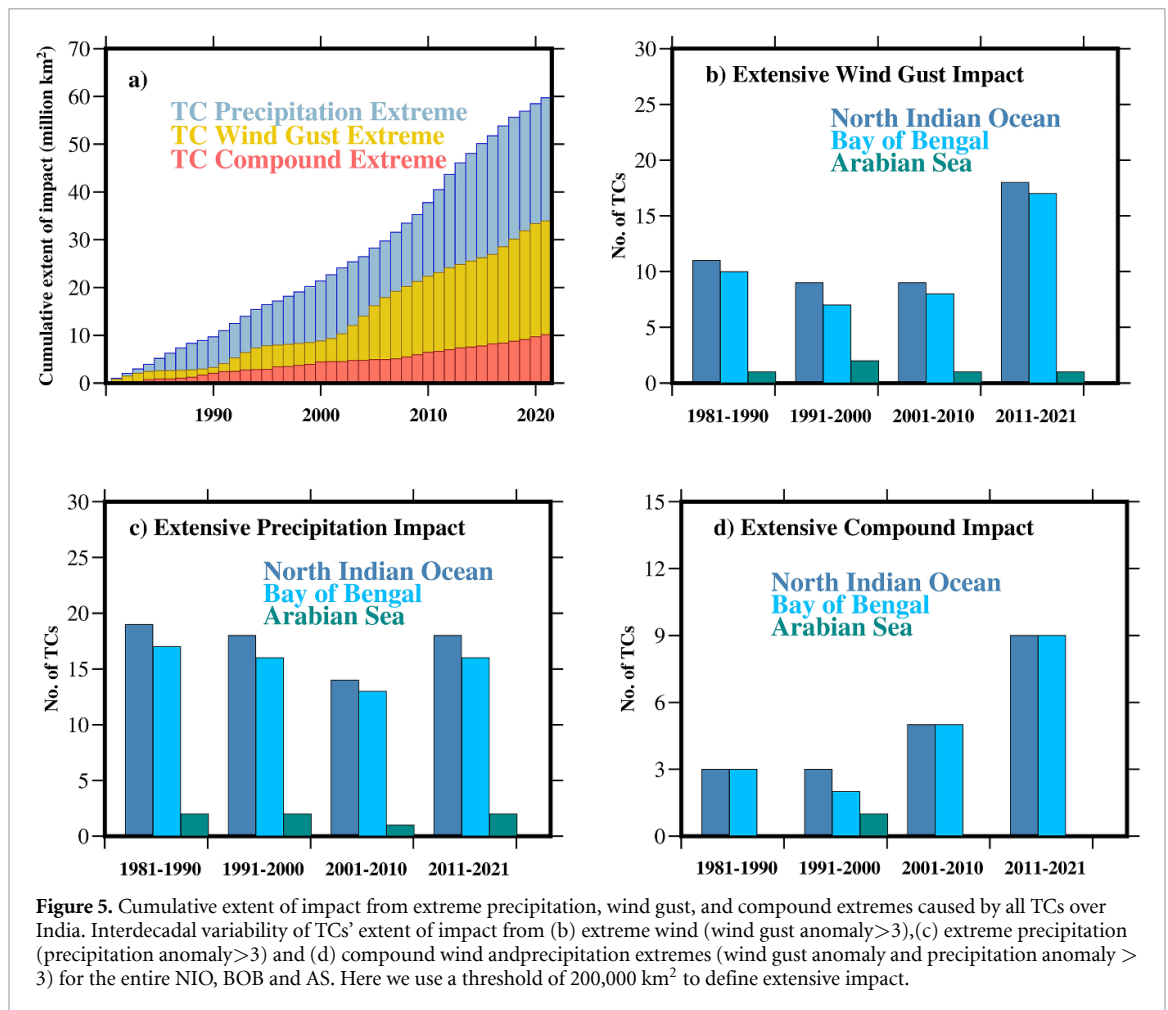
Based on the compound impact of precipitation and wind gust, we identified the five worst TCs that made landfall in the Indian region. Of this, the May 1999 TC (ESCS) had the highest joint return period and can be considered to be the worst, followed by TC Hudhud (240 years, ESCS), May 1990 TC (126 years, SuCS), TC Laila (88 years, SCS) and TC Amphan (71 years, SuCS). We find that the compound intensity of the TCs based on the joint return period does not follow the sustained wind speed-based index, which is currently the norm and can lead to a considerable underestimation of TC impact. Therefore, to assess TC hazards, both wind speed and precipitation should be considered.

3.3. Interdecadal variation in TCs

Next, we examined the interdecadal variation in all the TCs that made landfall over India. Subsequently, we analyzed the interdecadal distribution of TCs with extreme wind gusts, extreme precipitation, and compound extremes of wind gusts and rainfall. We identified 94 TCs from the NIO that made landfall in India from 1981 to 2021 (figure 1(a)). A total of 31 TCs made landfall over India during 1981–1990, out of which 29 originated from the BoB while only two from the AS. During 1991–2000, the number of TCs was 23, with 19 from the BoB and four from the AS. However, during 2001–2010 the number of TCs in the region fell to 16, with 13 from the BoB. From 2011 to 2021, the total number of TCs was 24, with 22 in the BoB. We find an overall decreasing trend in the total number of TCs in the NIO, which is consistent with previous studies (Balaji *et al* 2018, Singh *et al* 2019, Baburaj *et al* 2020).

The interdecadal distribution of TCs with extreme wind gusts in the AS, BoB, and the entire NIO is shown in figure 1(b). TCs with extreme wind gusts correspond to those TCs having a daily wind gust return period of 10 years or higher. The number of TCs with extreme wind gust in the NIO remained constant at about three during 1981–1990, 1991–2000, and 2001–2010. However, during the most recent decade (2011–2021), such TCs have increased four times compared to the previous decades (figures 1(b) and S1(a)). Moreover, TCs with extreme wind gust mainly originate from the BoB. The large number of TCs with extreme wind gust in BoB may be due to the higher frequency of TC generation. On the other hand, TCs from the AS have relatively higher intensity but a lower frequency of formation.

Next, we examined the decadal distribution of TCs with extreme precipitation in the AS, BoB, and NIO (figures 1(c) and S1(b)). TCs with extreme precipitation signify those having extreme daily rainfall with a ten year return period or higher. Our results show that the number of TCs with extreme rainfall in the NIO in the recent decade is substantially higher than in the previous decades. Except from 1981 to 1990, most TCs with extreme rainfall originated from the BoB. The low frequency of TCs with extreme precipitation in the AS may be primarily due to the lower frequency of cyclogenesis (Singh *et al* 2001, Evan and Camargo 2011). Since the AS's average sea surface temperature (SST) is less than that of the BoB (Jaswal *et al* 2012), the moisture uptake during TCs may not be large enough to cause significant rainfall over land (Knutson *et al* 2010). The number of TCs with extreme precipitation is higher than TCs with extreme wind gust during the 1981–1990 and 2001–2010, particularly in the BoB. This variation is significant as cyclone classification and



warnings are based on wind speed alone and do not consider extreme rainfall associated with TCs, which can underestimate the potential risk of extreme precipitation and flooding related to many TCs.

We analyzed the decadal distribution of TCs with compound precipitation and wind gust extremes in the AS, BoB, and NIO (figures 1(d), S1(c) and S3). The TCs with compound extremes have a joint return period of 10 years or higher. Despite an overall decreasing trend in total TC frequency in the NIO, we find an increase in TCs with compound extremes of precipitation and wind gust over the decades, with a significant rise in such TCs in the recent decade (2011–2021). During 2011–2021, half of the TCs in the NIO were TCs with compound precipitation and wind extremes compared to the 31 TCs during 1981–1990, out of which only four were associated with such extremes. We find similar trends in the BoB, where the total number of TCs in each decade has mostly stayed the same, while the number of TCs having compound extremes per decade has increased over time. Overall, we observe no significant trend in the number of TCs with compound extremes in the AS. Moreover, we note that the recent rise in compound extremes associated with TCs is consistent for varying TC extents (figure S1).

3.4. Interdecadal variation in the spatial distribution of TCs

To understand the change in the distribution of TCs over time in terms of compound wind and precipitation extremes, we estimated the cumulative extent of impact covered by extreme wind, precipitation and their compound extremes. Moreover, the decadal frequency of TCs from NIO, BOB and AS that had extreme wind gust covering a large area (>200 000 km²) is shown in figure (b). We find that the frequency of such TCs in NIO during 1981–1990, 1991–2000 and 2001–2010 remained relatively high. However, the decade 2011–2021 shows a considerable increase in the number of such TCs, with the frequency nearly doubling in the recent decade compared to the previous decades. A similar pattern is observed when considering only BOB TCs, with the recent decade showing a rise in the number of TCs compared to the previous three decades. We find no such trend when considering TCs that originate from AS.

We estimated the decadal frequency of TCs from NIO, BOB and AS with extreme precipitation extending over a vast region (>200 000 km²) (figure 5(c)). The number of TCs in NIO per decade did not vary

significantly during the 1981–2021 period apart from a slight decrease in the frequency during 2001–2010. In the case of BOB TCs, the TC frequency with rainfall extent greater than 200 000 km² remains more or less constant. Finally, for AS TCs, we find a similar pattern, but the number of TCs per decade is lower compared to BOB, which can be attributed to the lower frequency of TC formation in the AS.

We estimated the decadal variation in the frequency of TCs in NIO, BOB and AS having compound wind and precipitation extremes extending over an area greater than 200 000 km² (figure 5(d)). The total number of such TCs in the NIO shows a gradual rise over the decades with a three-fold increase in the frequency of such TCs in the recent decade compared to the 1981–1990 period. Moreover, the increase in TC frequency with extensive compound extreme coverage over the NIO is mainly driven by the BOB TCs. The TCs from AS was not associated with a large area of compound wind and precipitation extremes, except the May 1999 TC. Therefore, the rising frequency of larger TCs in terms of compound wind and precipitation extremes is particularly hazardous for the regions along the eastern coast of India.

4. Discussion

Due to its long coastlines, India is frequently affected by TCs originating in the NIO (National Disaster Management Authority 2008). However, the impact of compound wind and precipitation extremes in the region due to TCs needs to be better understood. We compared the univariate return periods of precipitation and wind gust of TCs with their copula-based joint return periods. Our results show that the frequency of TCs with the extreme wind remains constant from 1981 to 2010 in NIO but has increased in the recent decade. We find that in the NIO, most TCs with extreme precipitation originate from the BoB. We see an increasing trend in the frequency of TCs with extreme rainfall. Based on the TCs having compound wind and precipitation extremes in the NIO, we find a rising trend, with the recent decade showing a three-fold rise compared to 1981–1990. This increasing trend in the frequency of TCs with extreme wind and precipitation is consistent with previous studies, which show an increase in the number of intense TCs while the overall TC frequency shows a general decreasing trend (Balaji *et al* 2018, Singh *et al* 2019, Baburaj *et al* 2020). However, previous studies did not examine the compound extremes driven by TCs over NIO.

Based on the spatial distribution of the TCs having the highest joint return periods, we find that a significantly large region is affected by compound wind and precipitation extremes during each TC. We find that for most TCs, the area of extreme precipitation is relatively lesser than the region affected by extreme wind. Moreover, the wind speed of a TC reduces quickly after landfall. In most cases, the coastal area is the most affected by TC-induced compound wind and precipitation extremes. However, previous studies reported that TC rainfall within 100 km of TC centers is likely to increase under the warming climate (Knutson *et al* 2010, Grossmann and Morgan 2011, Walsh *et al* 2015). The mean TC lifetime in wind speed is projected under different scenarios (Seneviratne *et al* 2021), suggesting that the TCs will retain high wind speed for an extended period after landfall. Such an increase in TC precipitation and lifetime can lead to inland regions being affected by TCs with compound wind and precipitation extremes. Finally, the interdecadal variation in the spatial distribution of extreme wind and precipitation, and their compound extremes, shows a three-fold increase in the frequency of TCs with large compound extreme regions in the recent decade when compared to 1981–1990. Since the frequency of TCs with large extreme precipitation extent remains more or less constant, the increase in the extreme compound area of TCs is primarily driven by the rise in the extreme wind extent of the TCs. This increase in extreme wind extent of TCs can be because TC size and intensity is primarily driven by the SST, and ocean warming can lead to an increase in TC size and their rapid intensification (Sun *et al* 2017). Hence, this increasing trend in the frequency of larger TCs in terms of compound extremes can be attributed to a rise in SST over NIO, with larger regions being affected over time.

5. Conclusion

Based on our findings, the following conclusions can be made:

1. The frequency of TCs in the NIO with compound wind and precipitation is higher than that with only wind extremes from 1981 to 2010, indicating an underestimation of severe TCs when only wind gust is used.
2. The frequency of TCs with compound wind and precipitation extremes in the NIO exhibited a three-fold rise in the recent decade compared to 1981–1990.
3. A significantly large area along the coast is affected by compound wind and precipitation extremes of TCs. However, areas further inland are susceptible to TCs with such compound extremes.

- The frequency of TCs associated with large area of impact ($>200\,000\text{ km}^2$) of compound wind and precipitation extremes in the NIO shows a three-fold increase in the recent decade compared to 1981–1990. We find the TC size, in terms of compound wind and precipitation extreme, has increased during the recent decades.

Data availability statement

The data that support the findings of this study are openly available at the following URL/DOI: <https://cds.climate.copernicus.eu/cdsapp#!/dataset/reanalysis-era5-single-levels>.

Acknowledgments

The authors acknowledge the funding from the Ministry of Earth Sciences (MoES) under the Monsoon Mission. The cyclone tracks are freely available from the Cyclone eAtlas-IMD <http://14.139.191.203/AboutEAtlas.aspx>.

ORCID iDs

Akshay Rajeev  <https://orcid.org/0000-0003-0337-9450>

Vimal Mishra  <https://orcid.org/0000-0002-3046-6296>

References

- Anderson W B, Seager R, Baethgen W, Cane M and You L 2019 Synchronous crop failures and climate-forced production variability *Sci. Adv.* **5** eaaw1976
- Baburaj P P, Abhilash S, Mohankumar K and Sahai A K 2020 On the epochal variability in the frequency of cyclones during the pre-onset and onset phases of the monsoon over the North Indian Ocean *Adv. Atmos. Sci.* **37** 634–51
- Balaji M, Chakraborty A and Mandal M 2018 Changes in tropical cyclone activity in the north Indian Ocean during satellite era (1981–2014) *Int. J. Climatol.* **38** 2819–37
- Barton Y, Giannakaki P, von Waldow H, Chevalier C, Pfahl S and Martius O 2016 Clustering of regional-scale extreme precipitation events in Southern Switzerland *Mon. Weather Rev.* **144** 347–69
- Bevacqua E, Maraun D, Voudoukas M I, Voukouvalas E, Vrac M, Mentaschi L and Widmann M 2019 Higher probability of compound flooding from precipitation and storm surge in Europe under anthropogenic climate change *Sci. Adv.* **5** eaaw5531
- Bevacqua E, Voudoukas M I, Zappa G, Hodges K, Shepherd T G, Maraun D, Mentaschi L and Feyen L 2020 More meteorological events that drive compound coastal flooding are projected under climate change *Commun. Earth Environ.* **1** 1–11
- Cyclone eAtlas-IMD 2021 WEB Cyclone ATLAS:: about EAtlas (available at: <http://14.139.191.203/AboutEAtlas.aspx>) (Accessed 21 June 2021)
- Evan A T and Camargo S J 2011 A climatology of Arabian Sea cyclonic storms *J. Clim.* **24** 140–58
- Garg S and Mishra V 2019 Role of extreme precipitation and initial hydrologic conditions on floods in Godavari river basin, India *Water Resour. Res.* **55** 9191–210
- Grams C M, Binder H, Pfahl S, Piaget N and Wernli H 2014 Atmospheric processes triggering the central European floods in June 2013 *Nat. Hazards Earth Syst. Sci.* **14** 1691–702
- Grossmann I and Morgan M G 2011 Tropical cyclones, climate change, and scientific uncertainty: what do we know, what does it mean, and what should be done? *Clim. Change* **108** 543–79
- Guzzetti F, Peruccacci S, Rossi M and Stark C P 2008 The rainfall intensity–duration control of shallow landslides and debris flows: an update *Landslides* **5** 3–17
- Hao Z, Singh V P and Hao F 2018 Compound extremes in hydroclimatology: a review *Water* **10** 718
- Hendry A, Haigh I D, Nicholls R J, Winter H, Neal R, Wahl T, Joly-Laugel A and Darby S E 2019 Assessing the characteristics and drivers of compound flooding events around the UK coast *Hydrol. Earth Syst. Sci.* **23** 3117–39
- Jaswal A, Singh V and Bhambak S 2012 Relationship between sea surface temperature and surface air temperature over Arabian Sea, Bay of Bengal and Indian Ocean *Indian Geophys. Union* **16** 41–53
- Kim D, Ho C-H, Park D-S R and Kim J 2019 Influence of vertical wind shear on wind- and rainfall areas of tropical cyclones making landfall over South Korea *PLoS One* **14** e0209885
- Kimball S K 2008 Structure and evolution of rainfall in numerically simulated landfalling hurricanes *Mon. Weather Rev.* **136** 3822–47
- Klawns M and Ulbrich U 2003 A model for the estimation of storm losses and the identification of severe winter storms in Germany *Nat. Hazards Earth Syst. Sci.* **3** 725–32
- Knutson T R, McBride J L, Chan J, Emanuel K, Holland G, Landsea C, Held I, Kossin J P, Srivastava A K and Sugi M 2010 Tropical cyclones and climate change *Nat. Geosci.* **3** 157–63
- Li H, Wang D, Singh V P, Wang Y, Wu J, Liu J, Zou Y, He R and Zhang J 2019 Non-stationary frequency analysis of annual extreme rainfall volume and intensity using Archimedean copulas: a case study in eastern China *J. Hydrol.* **571** 114–31
- Mailier P J, Stephenson D B, Ferro C A T and Hodges K I 2006 Serial clustering of extratropical cyclones *Mon. Weather Rev.* **134** 2224–40
- Martius O *et al* 2013 The role of upper-level dynamics and surface processes for the Pakistan flood of July 2010: dynamics and surface processes of the Pakistan flood in 2010 *Q. J. R. Meteorol. Soc.* **139** 1780–97
- Martius O, Pfahl S and Chevalier C 2016 A global quantification of compound precipitation and wind extremes *Geophys. Res. Lett.* **43** 7709–17
- Matyas C J 2010 Associations between the size of hurricane rain fields at landfall and their surrounding environments *Meteorol. Atmos. Phys.* **106** 135–48

- Messmer M and Simmonds I 2021 Global analysis of cyclone-induced compound precipitation and wind extreme events *Weather Clim. Extremes* **32** 100324
- Nagler T *et al* 2021 VineCopula: statistical inference of vine copulas (available at: <https://cran.r-project.org/web/packages/VineCopula/VineCopula.pdf>)
- National Disaster Management Authority 2008 National disaster management guidelines (Government of India)
- Owen L E, Catto J L, Stephenson D B and Dunstone N J 2021 Compound precipitation and wind extremes over Europe and their relationship to extratropical cyclones *Weather Clim. Extremes* **33** 100342
- Raveh-Rubin S and Wernli H 2015 Large-scale wind and precipitation extremes in the Mediterranean: a climatological analysis for 1979–2012 *Q. J. R. Meteorol. Soc.* **141** 2404–17
- Rodgers E B and Pierce H F 1995 A satellite observational study of precipitation characteristics in Western North Pacific tropical cyclones *J. Appl. Meteorol. Climatol.* **34** 2587–99
- RSMC 1991 Report on cyclonic disturbances over North Indian Ocean during 1990 *Annual RSMC Report* (India meteorological department: New Delhi)
- RSMC 2000 Report on cyclonic disturbances over North Indian Ocean during 1999 *Annual RSMC Report* (India meteorological department: New Delhi)
- RSMC 2011 Report on cyclonic disturbances over North Indian Ocean during 2010 *Annual RSMC Report* (India meteorological department: New Delhi)
- RSMC 2015 Report on cyclonic disturbances over North Indian Ocean during 2014 *Annual RSMC Report* (India meteorological department: New Delhi)
- RSMC 2021 Report on cyclonic disturbances over North Indian Ocean during 2020 *Annual RSMC Report* (India meteorological department: New Delhi)
- Seneviratne S I *et al* 2021. Weather and climate extreme events in a changing climate *Climate Change 2021: The Physical Science Basis. Contribution of Working Group I to the Sixth Assessment Report of the Intergovernmental Panel on Climate Change* Intergovernmental Panel on Climate Change Ed *et al* (Cambridge University Press, Cambridge, United Kingdom)
- Seneviratne S *et al* 2012 Changes in climate extremes and their impacts on the natural physical environment pp 109–230 (<https://doi.org/10.7916/d8-6nbt-s431>)
- Singh D, Seager R, Cook B I, Cane M, Ting M, Cook E and Davis M 2018 Climate and the global famine of 1876–78 *J. Clim.* **31** 9445–67
- Singh K, Panda J, Sahoo M and Mohapatra M 2019 Variability in tropical cyclone climatology over North Indian Ocean during the period 1891–2015 *Asia-Pac. J. Atmos. Sci.* **55** 269–87
- Singh O P, Khan T M A and Rahman M S 2001 Has the frequency of intense tropical cyclones increased in the north Indian Ocean? *Curr. Sci.* **80** 575–80
- Sun Y, Zhong Z, Li T, Yi L, Hu Y, Wan H, Chen H, Liao Q, Ma C and Li Q 2017 Impact of ocean warming on tropical cyclone size and its destructiveness *Sci. Rep.* **7** 8154
- Walsh K J E *et al* 2015 Tropical cyclones and climate change *WIREs Clim. Change* **7** 65–89
- World Meteorological Organization 2020 Tropical Cyclones (available at: <https://public.wmo.int/en/our-mandate/focus-areas/natural-hazards-and-disaster-risk-reduction/tropical-cyclones>) (Accessed 22 October 2021)
- Ye Y and Fang W 2018 Estimation of the compound hazard severity of tropical cyclones over coastal China during 1949–2011 with copula function *Nat. Hazards* **93** 887–903
- Zhang X, Alexander L, Hegerl G C, Jones P, Tank A K, Peterson T C, Trewin B and Zwiers F W 2011 Indices for monitoring changes in extremes based on daily temperature and precipitation data *WIREs Clim. Change* **2** 851–70
- Zhang Y, Sun X and Chen C 2021 Characteristics of concurrent precipitation and wind speed extremes in China *Weather Clim. Extremes* **32** 100322
- Zscheischler J *et al* 2020 A typology of compound weather and climate events *Nat. Rev. Earth Environ.* **1** 333–47
- Zscheischler J, Naveau P, Martius O, Engelke S and Raible C C 2021 Evaluating the dependence structure of compound precipitation and wind speed extremes *Earth Syst. Dyn.* **12** 1–16